On the prediction of X-ray dose deviations and the influence of CT scan protocols

Freek CP du Plessis[1,a]

[1]*Department of Medical Physics, University of the Free State, P.O. Box 339, Bloemfontein, 9300, South Africa*
[a]*E-mail address: Duplessisfcp@ufs.ac.za*

Abstract

Patients undergoing computerized tomography (CT) scans for tumor localization and treatment planning are frequently scanned using pre-set customized exposure protocols for optimal imaging of different anatomical sites. The question arises if these scanning protocols will produce a deviation in the Hounsfield number for a given tissue that can afterwards be used to predict the resulting dose calculation deviation due to this. The question is also if the deviation in the Hounsfield number of a tissue is large enough to affect dose calculation clinically significant.

A study was devised in which a RMI phantom was scanned with five different scanning protocols and two CT beam energies at 120 and 135 kV. To assess the effect of insert configuration, Hounsfield number measurements were repeated for high density RMI inserts in the center and outer rings in the phantom. For each material insert the standard deviation of the Hounsfield number was calculated. To assist in dose prediction a series of DOSXYZnrc Monte Carlo calculations were carried out for beam qualities between 6 and 16 MV for a range of Hounsfield numbers calculated for bone and water. This provided information on how the depth dose varied as a function of Hounsfield number variation. Lastly, a series of treatment plans were setup for absorbed dose calculation using the RMI insert electron densities vs Hounsfield relations measured above. The absorbed dose of corresponding plans with the largest Hounsfield number variation were subtracted to find the dose discrepancies.

It was found that the dose discrepancies in tissue types could be indicated by the deviation of the Hounsfield number due to different scanning protocols. The calculated dose difference were in all cases within 3%.

Key words: CT; dose; RMI; scanning protocol; Monte Carlo.

Introduction

Cancer patients may have to be CT scanned for tumor localization before radiation treatment planning can begin. The quality of the treatment planning dose calculation will depend in the quality of the CT images imported into the treatment planning system (TPS). The CMS Xio TPS has the option of using the collapsed cone convolution algorithm. It makes use of relative electron densities (ED) of tissues for dose calculation. To extract this data from CT images, a phantom is scanned on the CT scanner to enable setting up the relative electron density vs Hounsfield unit (HU) curve or HU-ED curve. This phantom has different materials that can be arranged and have known relative ED. In the case of Monte Carlo (MC) dose simulation the CT data can be linked to material data with different physical density.

The relation between HU-ED depends on the kVp tube potential [1] and on the geometric arrangement of inserts used in a RMI-465 phantom [1,2]. Reconstructed HUs also depends on the type of phantom and arrangements of inserts [3,4]. For soft tissue the tube potential between 100 and 140 kVp does not alter the relation between relative ED and HU significantly although differences will be observed for bone > 160 HU [1].

To ensure that the CT data used in dose calculation is accurate relative to those used in relative electron density conversion, regular image quality testing are performed on the CT scanner.

In practice, there are circumstances where the standard scanner settings e.g. tube potential and tube current are not used during patient scanning, but rather a pre-set imaging protocol. For example the Toshiba Aquilion LB (large bore) CT scanner have five pre-set scan protocols namely: abdomen, chest, head-and-neck, head and pelvis scanning modes. The main difference between them is the tube current used which varies between 150 and 300 mAs.

The aim of this study was to predict dose differences in patients if different scanning protocols was used on a Toshiba Aquilion LB (large bore) CT scanner. As a further step Monte Carlo based DOSXYZnrc simulations were undertaken to determine how the dose in a material would change for a given change in its HU. This was established for bone and water. Afterwards the dose change per HU was used to compare to

dose differences in TPS dose calculations in patients for 6 MV beams.

Methods and Materials

CT number measurement

A RMI-465 electron density CT phantom (Gammex, Wi, USA) with 20 material inserts that covers a range of electron densities was scanned on a Toshiba Aquilion LB CT scanner. Five scanning protocols were employed to scan the phantom. The scanning protocols included an abdomen, chest, head-and-neck, head and pelvis scanning mode. Each of these scanning protocols has a tube potential of 120 kVp with tube current settings of: 150, 150, 225, 300, and 263 mAs respectively. These mAs settings were also used for the scanning protocols, but this time a tube potential of 135 kVp was used. The resulting reconstructed Hounsfield numbers for the phantom inserts were compared among the different scanning protocols and the standard deviation of the Hounsfield numbers were calculated for each insert material.

The effect of scanning protocol also included different configurations of inserts in the RMI 465 phantom. In one case the dense inserts were arranged on the outside ring (DO) and the less dense inserts in the inside ring of the RMI phantom. In another case the arrangement was swapped so that the dense inserts were on the inner ring (DI) of the phantom.

Monte Carlo investigations

To understand how the local dose on the central axis can be influenced through a variation in Hounsfield number, a MC study was designed to investigate the local percentage dose variation for a range of physical densities of water and ICRPbone. The DOSXYZnrc code was used and available photon energy spectra between 4 and 16 MeV included in the BEAMnrc Monte Carlo code were adopted as input spectra. Homogeneous phantoms were constructed consisting of water with densities of 1.0, 1.02, 1.05, 1.07, and 1.10 g/cm^3 that corresponded to CT values of 0, 13, 46, 68, and 102 HU respectively. The ICRPbone material densities were set to: 1.2, 1.5, 1.8, 2.0, 2.5 corresponding to CT numbers of 756, 946, 1546, 1946, and 2946 HU respectively. These were calculated from the HU-to-electron density conversion curve used in the CMS XIO TPS.

The phantom dimensions were $20 \times 20 \times 30$ cm^3, with a depth resolution (z) of 0.25 cm. The x and y resolution was 1×1 cm^2. The number of histories was set to 3×10^8. After each simulation the percentage depth dose were extracted and smoothed through exponential fitting for all dose values beyond the maximum dose depth. The smoothed depth dose data were used to derive relative percentage depth dose values

for the case of different water and ICRPbone densities respectively. Since Hounsfield numbers could be assigned to each percentage depth dose curve, the change in HU per unit depth dose, $M(z) = \Delta CT/\Delta PDD(z)$ could be calculated. Here $M(z)$ is a gradient value showing the change in CT number ΔCT for a corresponding change in the local percentage depth dose $\Delta PDD(z)$. This data set were calculated for water and ICRP bone at the mentioned beam energies. For each case a box-and-whisker plot was obtained to investigate how $M(z)$ varies over depth for each material density. An average value for $M(z)$ at each beam energy and material were established that would show the variation of Hounsfield number to obtain a 1 percent local dose difference.

Dose calculation with different CT data conversion sets

The HU-ED conversion curves for each scanning protocol in the CT number measurement section above were used to convert CT data into relative ED images prior to dose calculation. The ED *vs* HU conversion curves were imported into a Xio treatment planning system (TPS) and the dose distribution were calculated using the collapsed cone convolution (CCC) algorithm for head-and-neck, head and prostate cases. In each case the HU-ED conversion curve were used for each scanning protocol to convert the patient CT data before the absorbed dose distribution was calculated. Afterwards the largest dose deviation between the scanning protocols were used to set up 2-D percentage dose difference maps for the three treatment cases.

Results

Tables 1-4 show calculated Hounsfield numbers for RMI inserts obtained from five scanning protocols at 120 kVp and 135 kVp. They were measured on a Toshiba Aquilion LB scanner for cases were the high density inserts were inserted on the outer ring and the inner most ring in the RMI phantom respectively.

Figure 1 shows a set of graphs showing $\Delta CT(z)$ for different densities of water and ICRPbone between photon spectra ranging between 6 and 16 MV. The box-and-whisker graphs indicate that the values for $\Delta CT(z)$ between the first and third quartile is higher in bone compared to water. From the top three graphs it can be deduced that a value of $\Delta CT = 30$ HU would be reasonable to take as the allowed fluctuation in CT number that would cause a dose variation of within one percent. For the corresponding case for bone $\Delta CT = 100$ HU is chosen from the results.

Table 1. Hounsfield numbers calculated from 120 kVp scans using the five scanning protocols in the case where the dense inserts were on the outside ring (DO) in the RMI phantom.

120 kVp		High densities outside				
Scan protocol		Abdomen	Chest	Head and neck	Head (prone)	Pelvis
Tube current (mAs)		150	150	225	300	263
Material	Relative electron density	Hounsfield number				
Lung (300)	0.292	-710.1	-698.1	-724.8	-712.9	-742.2
Lung (450)	0.438	-648.1	-667.3	-668.3	-672.9	-667.2
Adipose	0.895	-88.7	-84.3	-87.6	-84	-86.2
Polyethylene	0.945	-73.8	-75.5	-80.8	-80.3	-74.0
Breast	0.980	-39.8	-39.5	-37.7	-41.7	-32.8
Solid water	1.000	2.8	-6.2	3.8	2.3	4.1
Brain	1.039	25.6	22.3	27.8	30.1	25.7
Liver	1.116	105.9	100.1	98.0	95.6	97.9
Inner bone	1.081	213.1	223.8	217.7	225.4	223.2
Bone mineral	1.099	231.4	244.7	247.1	239.8	241.7
ResinCB4	1.147	112.5	105.3	111.4	109.6	113.2
$CaCO_3$(10%)	1.142	173.6	174.9	175.5	173.6	172.3
Acrylic	1.050	119.1	128.3	132.8	131.5	129.7
$CaCO_3$(30%)	1.285	449.6	475.1	472.6	476.0	473.9
$CaCO_3$(50%)	1.473	853.2	864.5	859.8	861.3	861.4
Cortical bone	1.707	1266.2	1295.9	1298.1	1289.5	1293.0

Table 2. Hounsfield numbers calculated from 135 kVp scans using the five scanning protocols in the case where the dense inserts were on the outside ring (DO) in the RMI phantom.

135 kVp		High densities outside				
Scan protocol		Abdomen	Chest	Head and neck	Head (prone)	Pelvis
Tube current (mAs)		150	150	225	300	263
Material	Relative electron density	Hounsfield number				
Lung (300)	0.292	-688.3	-725.0	-723.7	-779.9	-707.1
Lung (450)	0.438	-628	-647.7	-655.0	-716.2	-636.1
Adipose	0.895	-85.6	-78.3	-82.3	-73.1	-102.0
Polyethylene	0.945	-75.3	-74.0	-70.8	-68.0	-86.6
Breast	0.980	-47.1	-36.3	-36.3	-36.9	-66.6
Solid water	1.000	9.8	7.2	3.0	-7.2	-0.6
Brain	1.039	18.6	22.8	26.6	18.4	13.8
Liver	1.116	94.3	94.6	99.9	73.8	94.5
Inner bone	1.081	202.0	203.5	204.1	169.9	118.3
Bone mineral	1.099	208.3	215.7	222.0	187.9	194.0
ResinCB4	1.147	96.3	108.9	114.0	92.1	94.7
$CaCO_3$(10%)	1.142	160.0	166.6	168.5	140.9	169.1
Acrylic	1.050	132.2	136	134.8	110.7	112.9
$CaCO_3$(30%)	1.285	421.9	433.2	445.4	730.1	412.1
$CaCO_3$(50%)	1.473	768.7	795.2	801.8	1218.9	731.1
Cortical bone	1.707	1175.3	1197.4	1203.1	1770.5	1127.2

Table 3. Hounsfield numbers calculated from 120kVp scans using the five scanning protocols in the case where the dense inserts were in the inside ring (DI) in the RMI phantom.

120 kVp		High densities inside				
Scan protocol		Abdomen	Chest	Head and neck	Head (prone)	Pelvis
Tube current (mAs)		150	150	225	300	263
Material	Relative electron density	Hounsfield number				
Lung (300)	0.292	-729.7	-721.0	-729.8	-711.7	-709.8
Lung (450)	0.438	-644.6	-649.6	-650.9	-656.3	-624.9
Adipose	0.895	-86.4	-88.1	-84.7	-95.1	-105.8
Polyethylene	0.945	-65.3	-69.7	-64.7	-68.9	-67.8
Breast	0.980	-33.6	-38.1	-46.6	-52.9	-76.6
Solid water	1.000	2.9	2.7	-1.7	0.4	-8.7
Brain	1.039	29.6	25.6	21.7	11.4	17.2
Liver	1.116	79.5	85.5	84.4	61.5	67.1
Inner bone	1.081	208.8	216.7	202	184.7	183.5
Bone mineral	1.099	228.0	231	228	191.3	206.2
ResinCB4	1.147	112.0	109.2	102.8	90.8	103.9
$CaCO_3(10\%)$	1.142	173.7	172.7	163.3	138.2	160.0
Acrylic	1.050	123.9	128.3	119.8	95.0	113.8
$CaCO_3(30\%)$	1.285	455.6	465.6	456.4	544.9	425.9
$CaCO_3(50\%)$	1.473	849.2	855.2	846.8	1031	789.7
Cortical bone	1.707	1249	1253.1	1255	1500	1134.8

Table 4. Hounsfield numbers calculated from 135 kVp scans using the five scanning protocols in the case where the dense inserts were in the inside ring (DI) in the RMI phantom.

135 kVp		High densities inside				
Scan protocol		Abdomen	Chest	Head and neck	Head (prone)	Pelvis
Tube current (mAs)		150	150	225	300	263
Material	Relative electron density	Hounsfield number				
Lung (300)	0.292	-738	-732.4	-787	-752.5	-764.2
Lung (450)	0.438	-645.7	-645.0	-708.8	-692.8	-646.8
Adipose	0.895	-86.6	-79.5	-76.6	-83.7	-161.7
Polyethylene	0.945	-70.2	-59.7	-69.6	-91.1	-77.3
Breast	0.980	-36.5	-35.6	-34.2	-47.1	-38.0
Solid water	1.000	5.5	5.4	-8.2	-2.3	9.2
Brain	1.039	24.8	28.1	20.0	4.9	23.3
Liver	1.116	91.1	89.3	71.5	86.2	122.3
Inner bone	1.081	222.1	201	168.5	253.2	206
Bone mineral	1.099	237.8	217.7	185.7	284.5	293.3
ResinCB4	1.147	111	115.8	91.7	93.6	103.2
$CaCO_3(10\%)$	1.142	178.3	168.4	138.9	183.1	227.6
Acrylic	1.050	132.6	137.5	112.0	123.5	115
$CaCO_3(30\%)$	1.285	473	440.4	726.1	649.6	413.7
$CaCO_3(50\%)$	1.473	867.2	806	1226	1232.1	1028.8
Cortical bone	1.707	1281.8	1277.6	1785.6	1879.9	1382.5

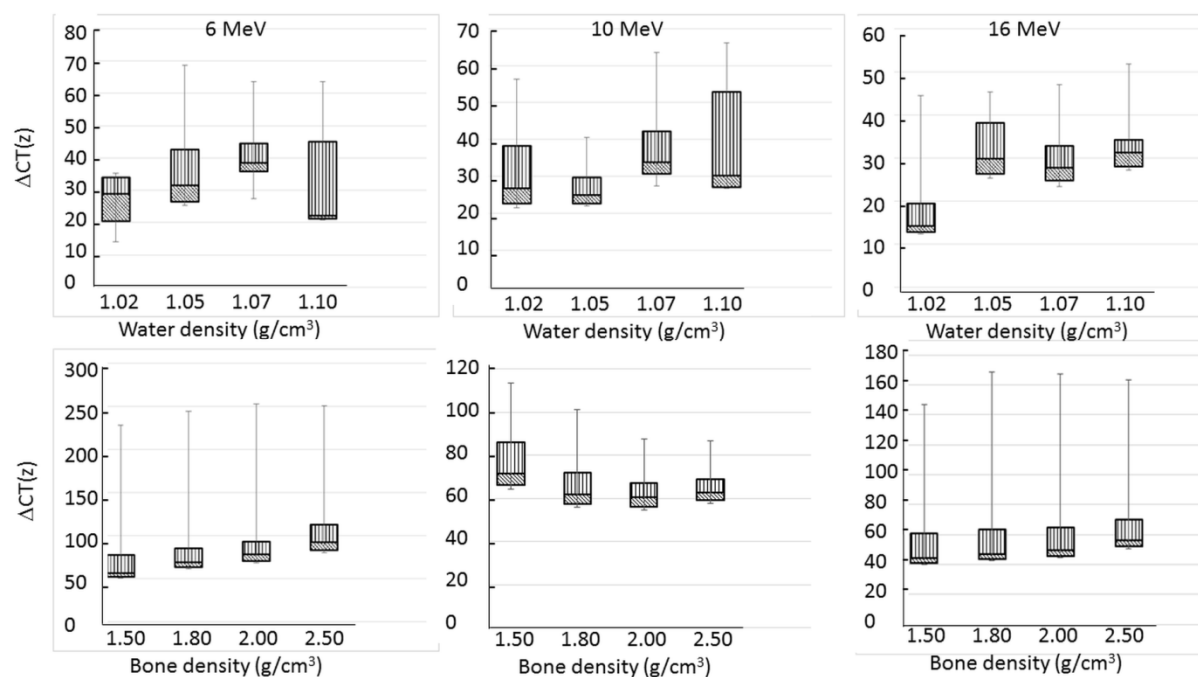**Figure 1. ΔCT(z) vs various densities for water (top row) and ICRPbone (bottom row). It is evaluated for three energies; 6 MeV (first column), 10 MeV (second column), and 16 MeV (third column).**

The value of ΔCT(z) in **Figure 1** shows the amount that the Hounsfied number can vary per unit percentage depth dose variation. Thus from the choice of M(z) from the above MC simulation data the dose variation due to a variation in CT number is defined as:

$$\Delta D = \frac{\Delta CT}{M} \qquad \text{Eq. 1}$$

Equation 1 allows the calculation of the dose variation (ΔD) due to a variation in Hounsfield number (ΔCT). Constant M is defined as 30 HU for soft tissue. Our studies have shown that for a 0.05 unit density variation in lung the above CT number range is also valid. As a result, **Equation 1** can also be used to calculate the variation in dose in lung for a given variation in CT numbers.

Table 5 shows the standard deviation of the CT numbers (noted in **Tables 1-4**) of each material as they vary over the chosen scanning protocol. The four cases (two scanning energies and two insert arrangements) are presented in **Table 5**. At the 135 kVp scanning tube potential there is a larger standard deviation in CT number that is observed for the higer relative electron density materials compared to the same data at 120 kVp. Using **Equation 1** the predicted standard dose deviation was calculated and tabulated in **Table 6**. We see a variety of cases from which the predicted dose deviation exceeds one percent for the inserts configurations and scanning tube potentials. For the DO configuration, at 120 kVp, all dose deviations are within 0.6 percent where the biggest discrepancy is for low density lung 300. If the tube potential is increased to 135 kVp then lung 450, inner bone, CaCO₃ (30 and 50%), and cortical bone experience dose deviations larger than one percent. For the DI configuration at 120 kVp again only

cortical bone shows a dose deviation exceeding one percent. At 135 kVp the dose deviations exceeding one percent it present for virtually all materials at the same tube potential for the DO configuration. Therefore it is expected that bone-like structures scanned at 135 kVp would result in the largest dose discrepancy in dose calculation using this relative electron (ED) *vs* CT number conversion table. Extreme cases were reported for a Head and Neck case, a Head case, and four field prostate case.

Table 5. The standard deviation of the CT numbers for each insert taken over the five scanning protocols for each of the four scanning energy-density configurations (Tables 1-4).

Material	Relative electron density	STD dev of Hounsfield numbers for dense inserts outside (D O) and dense inserts inside (D I)			
		120 kVp D O	135 kVp D O	120 kVp D I	135 kVp D I
Lung (300)	0.292	16.7	29.7	9.5	21.9
Lung (450)	0.438	9.6	34.9	12.1	30.6
Adipose	0.895	2.0	11.0	8.7	36.0
Polyethylene	0.945	3.4	7.1	2.2	11.6
Breast	0.980	3.4	13.1	16.9	5.1
Solid water	1.000	4.3	6.7	4.8	7.0
Brain	1.039	2.9	4.9	7.1	9.0
Liver	1.116	3.9	10.1	10.7	18.6
Inner bone	1.081	5.1	37.2	14.7	31.0
Bone mineral	1.099	6.0	14.4	17.4	45.3
ResinCB4	1.147	3.2	9.6	8.2	10.5
CaCO₃(10%)	1.142	1.3	92.5	70.2	32.0
Acrylic	1.050	5.4	12.4	13.0	94.2
CaCO₃(30%)	1.285	11.2	135.6	44.6	138.7
CaCO₃(50%)	1.473	4.2	200.8	91.5	197.4
Cortical bone	1.707	12.9	267.7	134.0	312.7

The results were calculated from **Equation 1** using values for M obtained from MC simulations in bone, water and lung tissue. It is observed that the 135 kVp DI and DO arrangements for inserts give results in dose variations above one percent in bone as shown in cases for $CaCO_3(30\%)$, $CaCO_3(50\%)$, and cortical (dense) bone. It is thus hypothesized that these dose variations can occur in CT scanned data using different scanning protocols when dose is calculated for a standard ED vs HU curve.

To test this hypothesis, three cases were taken of patient scans for a head, head-and-neck, and abdominal cases. Here the CT data were converted into electron density using HU-ED conversion curves obtained from the Hounsfield number data in **Tables 1-4**. Dose differences were mapped for scanning protocols as indicated on **Figures 2-4**.

In **Figure 2** a whole brain treatment is shown obtained from two opposing lateral photon fields at 6 MV. The top left image shows the dose distribution calculated for electron densities obtained from the ED vs CT curve obtained using the 'HEAD prone' scanning protocol at 135 kVp. The top right image shows the same treatment plan but this time the absorbed dose was calculated for electron densities conversion using the 'Abdomen' scanning protocol at 135 kVp. The bottom right panel shows the percentage dose difference for the dose distributions. The indicated percentage dose difference is within 1.6 percent with the biggest differences observed in the bony structures of the skull and vertebrae regions. In **Table 6**

the predicted dose for different bone types is on average within the range of 1.4 to 3.1 percent for cortical bone for the 135 kVp data (both DO and DI). Brain tissue predicts dose difference data well less than one percent which falls in the blue range of the dose difference map, and this is observed in the percentage dose difference map in **Figure 2**. The predicted dose difference in brain is in the order of 0.3 percent as shown in **Table 6** for 135 kVp.

In **Figure 3** a Head-and-neck treatment case is presented for 6 MV photon beams. Again we see that the largest dose differences occurring with HU-to-ED conversions for the 135 kVp DI case. Dose differences predicted in **Table 6** shows that, as in the case for **Figure 1**, bone structures (vertebrae and skull) would have the largest dose discrepancy as shown in the bottom right panel in **Figure 3**. Here dose differences of up to 1.5 percent is shown on the dose difference map and predicted in **Table 6** for $CaCO_3(30\%)$ and $CaCO_3(50\%)$ which represents different densities of hard bone.

In **Figure 4** a Prostate treatment case is presented using a four field plan and 6 MV photon beams. The HU-ED conversions for the 135 kVp DO case is presented against CT data obtained at 135 kVp for the DI case, using the 'HEAD (prone)' scanning protocol. Here all dose differences are predicted in **Table 6** for the 135 DI data to be within one percent except in the bony anatomical regions where a slightly higher dose difference is predicted.
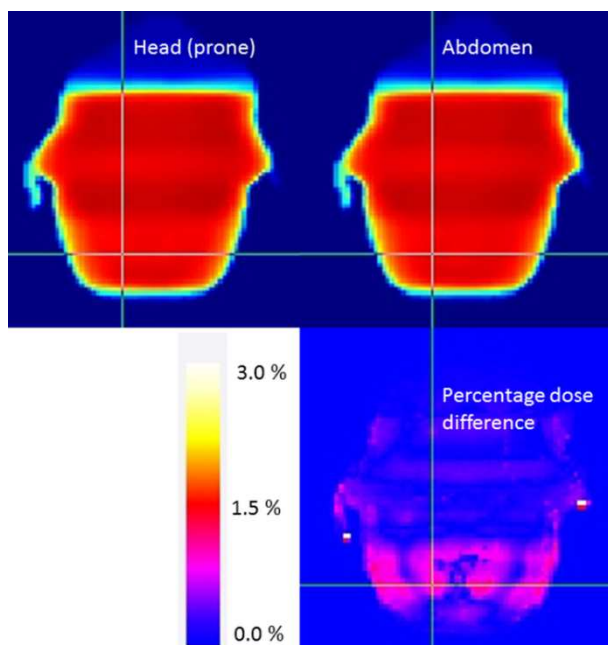

Figure 2. Radiation treatment planning for a Head treatment. In the top left panel the dose was calculated using the HU-ED curve obtained from the HEAD (prone) scan protocol and the top right panel is the dose calculated for the HU-ED curve obtained with the abdomen scan protocol of the RMI phantom. The bottom panels shows the percentage dose difference between these protocols. With the bottom left panel indicating the dose difference intensity scale.
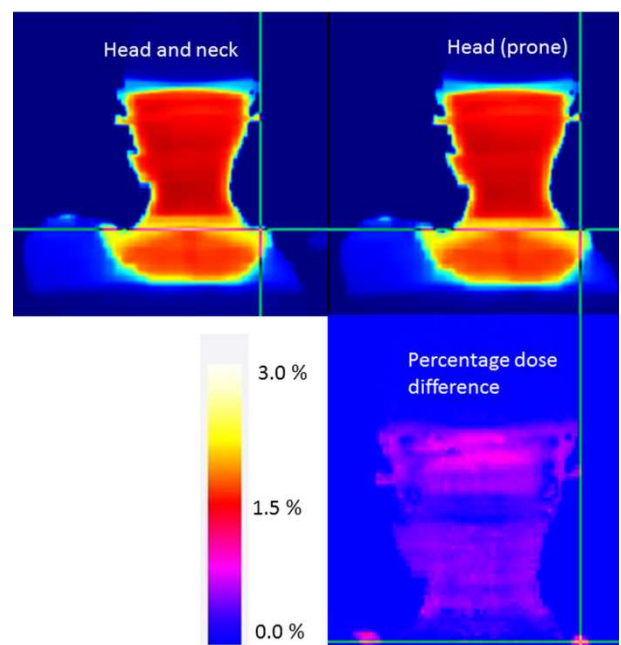

Figure 3. Radiation treatment planning for a Head and Neck treatment. In the top left panel the dose was calculated using the HU-ED curve obtained from the 'HEAD and Neck' scan protocol and the top right panel is the dose calculated using the HU-ED curve obtained with the 'HEAD prone' scan protocol. The bottom panels shows the percentage dose difference between these protocols along with its intensity scale.
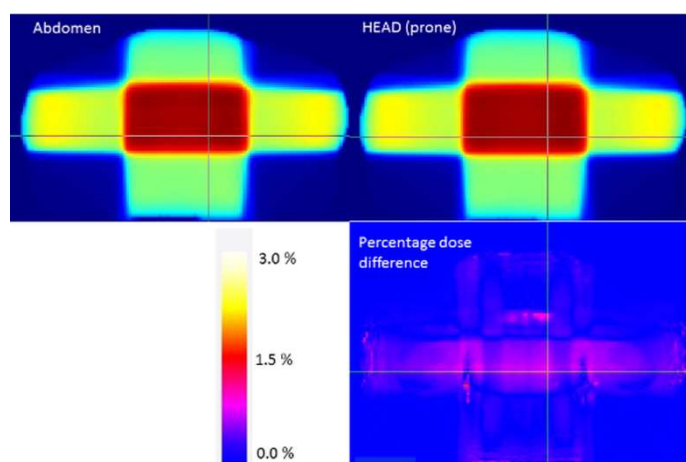
Figure 4. Radiation treatment planning for a prostate. In the top left panel the dose was calculated using the HU-ED curve obtained from the 'Abdomen' scan protocol and the top right panel is the dose calculated for electron densities obtained using a HU-ED conversion with the 'HEAD prone' scan protocol. This data was taken at 135 kVp. The bottom panels shows the percentage dose difference between these protocols with its intensity scale.

Table 6. Percentage dose deviation as calculated with Equation 1.

Material	M (HU)	Percentage deviation of dose (ΔD)			
		120 kVp D O	135 kVp D O	120 kVp D I	135 kVp D I
Lung (300)	30	0.6	0.8	0.3	0.7
Lung (450)	30	0.3	1.2	0.4	1.0
Adipose	30	0.1	0.4	0.3	1.2
Polyethylene	30	0.1	0.2	0.1	0.4
Breast	30	0.1	0.4	0.6	0.2
Solid water	30	0.1	0.2	0.2	0.2
Brain	30	0.1	0.2	0.2	0.3
Liver	30	0.1	0.3	0.4	0.6
Inner bone	30	0.2	1.2	0.5	1.0
Bone mineral	100	0.1	0.1	0.2	0.5
ResinCB4	100	0.0	0.1	0.1	0.1
$CaCO_3(10\%)$	100	0.0	0.9	0.7	0.3
Acrylic	100	0.1	0.1	0.1	0.9
$CaCO_3(30\%)$	100	0.1	1.4	0.4	1.4
$CaCO_3(50\%)$	100	0.0	2.0	0.9	2.0
Cortical bone	100	0.1	2.7	1.3	3.1

Discussion

It is custom to set up HU-ED curves for dose calculation purposes, since analytical dose calculation algorithms utilizes electron density data. In this study the HU-ED curves were measured on a RMI 450 phantom. The reconstructed Hounsfield numbers depend on the maximum tube potential (kVp), the configuration of inserts, and the scanning protocol as seen in **Tables 1-4**. In a study by Guan and co-workers they found that the calculated dose differs within 2% for a range of HU-ED curves, but they did not established the relation between dose difference and variations in Hounsfield number as set out in this study [5]. Our results are in general agreement with their conclusion about the dose variation vs HU-ED variation. Our biggest predicted dose difference is with bone at 135 kVp which is 3.1 percent. Our results also suggested that dose differences in bone is not clinically significant, albeit that our approach was founded on Hounsfield number variation and the resulting predicted dose variation based on Monte Carlo simulation in **Figure 1**.

To get an understanding of how the dose could vary with a variation in Hounsfield number a set of MC simulations were performed. And from these results it was deduced that these numbers could vary within 100 HU for bone and 30 HU for soft tissue to cause a dose variation of up to one percent. This was calculated for beam energies between 6 and 16 MeV.

The variation in Hounsfield number among the scanning protocols is shown in **Table 5**, from which the percentage dose deviation (ΔD) is calculated for each insert using **Equation 1**. **Equation 1** is formulated to predict the dose deviation among the inserts due to the standard deviation of the Hounsfield numbers over the five scanning protocols. CT numbers obtained at 135 kVp showed a larger deviation among the scanning protocols compared to their 120 kVp counterparts.

This indicates that at 120 kVp the scanning protocols would produce Hounsfield numbers with such small standard deviation for any insert that its overall dose effect should not exceed one percent. The only exception is for cortical bone where a dose deviation of 1.3 percent is predicted at 120 kVp for the configuration where the dense inserts is located in the inside ring (DI) of the RMI phantom. For data obtained at 135 kVp the dose deviation can increase from 1.4 to above 3 percent for bone materials due to the large deviation in Hounsfield numbers obtained over the scanning protocols. The insert configuration (DO vs DI) can cause variation in CT number at the same tube potential. For 120 kVp the difference in dose variation (ΔD) is 1.2 percent for cortical bone, since for the DI case ΔD = 1.3% and for the DO case its value is 0.1%. At 135 kVp this difference in dose variation between DI and DO is 3.1% – 2.7% = 0.4 %.

To test the predictive power of the dose deviation expected in different tissues three treatment planning cases were presented for head, head-and-neck, and prostate treatments using 6 MV beams on a Xio treatment planning system. For 3D-dose calculation, the dose deviation for each treatment tisue is predicted by **Table 6** and is observed for the bone structures in all three treatment cases. This means that the variation in measured HU-to-ED curve will lead to dose calculation variation within one percent in soft tissue if the patient is scanned at different scanning protocols. This is especially significant at the higher scanning energy of 135 kVp. Although different scanning protocols are presented on the Toshiba Aquilon LB CT scanner, it should not lead to large variation in dose calculation based on the reconstructed CT numbers at 120 kVp. Thus the effect on absorbed dose calculation can be calculated using **Equation 1** if the CT variation over different scanning protocols are known a priori.

Conclusion

CT numbers can vary when different scanning protocols are used to obtain anatomical information for treatment planning purposes. The degree of variation can influence the local calculated dose. A table that shows the variation of the CT numbers can be linked into the variation of dose. This was shown for three treatment plans where the biggest dose difference was in bone tissue over the different scanning protocols. The local dose difference in soft tissue and bone structures can be linked to the variation in CT numbers for RMI phantom inserts provided in **Table 6**. HU-to-ED curves measured at 135 kVp shows more inter-scan protocol variation compared to 120 kVp. The insert configuration can cause variation in CT number the effect it has on local dose variation is about 1.2 percent for cortical bone at 120 kVp. For 135 kVp this difference in dose is 0.4 percent.

References

[1] Nobah A, Moftah B, Tomic N, et al. Influence of electron density spatial distribution and X-ray beam quality during CT simulation on dose calculation accuracy. J Appl Clin Med Phys. 2011;12(3):80-89.

[2] Constantinou C, Harrington JC, DeWerd LA. An electron density calibration phantom for CT-based treatment planning computers. Med Phys. 1992;19(2):325-327.

[3] Inness EK, Moutrie V, Charles PH. The dependence of computed tomography number to relative electron density conversion on phantom geometry and its impact on planned dose. Australas Phys Eng Sci Med. 2014;37(2):385-391.

[4] Sande EPS, Martinsen ACT, Hole EO, et al. Interphantom and interscanner variations for Hounsfield units–establishment of reference values for HU in a commercial QA phantom. Phys Med Biol. 2010;55(17):5123-5135.

[5] Guan H, Yin FF, Kim JH. Accuracy of inhomogeneity correction in photon radiotherapy from CT scans with different settings. Phys Med Biol. 2002;47(17):N223-N231.